

VOLUMETRIC HARMONIC BRAIN MAPPING*

Yalin Wang¹, Xianfeng Gu², Tony F. Chan¹, Paul M. Thompson³, Shing-Tung Yau⁴

¹ Mathematics Department, UCLA

² CISE, University of Florida

³ Lab. of Neuro Imaging and Brain Research Institute, UCLA School of Medicine

⁴ Department of Mathematics, Harvard University

{ylwang,chan}@math.ucla.edu, gu@cise.ufl.edu, thompson@loni.ucla.edu, yau@math.harvard.edu

ABSTRACT

In [1], we developed two different techniques to study volume mapping problem in Computer Graphics. The first one is to find a harmonic map from a 3 manifold to a 3D solid sphere and the second is a sphere carving algorithm which calculates the simplicial decomposition of volume adapted to surfaces. In this paper, we apply these two techniques to brain mapping problem. We use a tetrahedral mesh to represent the brain volume. The experimental results on both synthetic and brain volume data are reported. We suggest that 3D harmonic mapping of brain volumes to a solid sphere can provide a canonical coordinate system for feature identification and segmentation, as well as anatomical normalization.

1. INTRODUCTION

The rapid growth in brain imaging technologies has been matched by an extraordinary increase in the number of investigations analyzing brain structure and function in clinical and research settings [2]. Brain surface conformal mapping research [3, 4] has been successful and this motivates our more general investigation of 3D volumetric brain harmonic mapping. The motivations for 3D volumetric brain mapping research are clear. The brain is inherently 3D, and besides the surface information, MRI also yields rich morphometric information for interior brain structures. By transforming the full 3D brain volume to a solid sphere, our goal is to investigate how features map into this canonical 3D coordinate system in the same way as 2D conformal flattening has helped in analyzing cortical surface geometry. Nonlinear mapping of two brain volumes to a sphere can also assist with the subsequent nonlinear registration of one brain volume to another.

For 3D brain volume transformation research, Thompson et al. [5] used weighted linear combinations of radial

functions, describing the influence of deforming surfaces on points in their vicinity, to extend a surface-based deformation to the whole brain volume for the purpose of registering a brain with another. Christensen et al. [6] present diffeomorphic transformations of three-dimensional anatomical image data using fluid deformation method. It forces a diffeomorphic transformation by tracking the Jacobian of the transformation. Gee [7] studied brain volume matching with a generalized elastic matching method within a probabilistic framework. The approach can resolve issues that are less naturally addressed in a continuum mechanical setting. Ferrant et al. [8] presented an algorithm for non-rigid registration of 3D MR intraoperative image sequences showing brain shift. The 3D anatomic deformation field, in which surfaces are embedded, is then inferred from the displacements at the boundary surfaces using a biomechanical finite element model for the constituent objects. Wang, Gu and Yau [1] proposed a general 3D volumetric harmonic mapping algorithm. The algorithm can work with manifolds with genus zero and non genus zero surfaces. They demonstrated their algorithm in object modeling and animation applications.

In 2D case, a harmonic map between two convex planar regions is diffeomorphic if and only if the restriction on the boundary is diffeomorphic. 3D harmonic map is much more complicated. In this paper, we construct a harmonic map in \mathbb{R}^3 with a heat flow method. First we conformally map the boundary of the 3D volume to a sphere, then minimizes the volumetric harmonic energy while keeping the surface fixed. To build volumetric brain data, we applied sphere carving algorithm of [1] to calculate the simplicial decomposition of volume adapted to surfaces. To the best of our knowledge, this is the first work to apply volumetric harmonic map to brain mapping problem. This work is also quite general and can easily be generalized to higher-dimensional cases.

The remainder of the paper is organized as follows. In Section 2, we give the definitions of harmonic energy and a detailed description of our algorithm. Section 3 reports our experiments on both synthetic and brain MRI image data. We conclude the paper with the discussion of future research directions in Section 4.

*ACCEPTED FOR PUBLICATION AND PRESENTATION AT ISBI 2004. THIS WORK WAS PARTIALLY SUPPORTED BY NATIONAL INSTITUTES OF HEALTH GRANTS R21 EB001561 AND R21 RR019771; NSF CONTRACT DMS-9973341, NSF CONTRACT ACI-0072112, ONR CONTRACT N00014-03-1-0888, AND NIH CONTRACT P20 MH65166.

2. VOLUMETRIC HARMONIC MAPPING ALGORITHM

2.1. Definitions

Suppose K is a simplicial complex, and $f : |K| \rightarrow \mathbb{R}^3$, which embeds $|K|$ in \mathbb{R}^3 ; then (K, f) is called a mesh. Given a genus zero tetrahedral mesh M , our goal is to compute its harmonic map to a sphere in \mathbb{R}^3 .

Definition 1 All piecewise linear functions defined on K form a linear space, denoted by $C^{PL}(K)$

Definition 2 Suppose a set of string constants $k(u, v)$ are assigned, then the inner product on C^{PL} is defined as the quadratic form:

$$\langle f, g \rangle = \frac{1}{2} \sum_{\{u, v\} \in K} k(u, v)(f(u) - f(v))(g(u) - g(v)) \quad (1)$$

The energy is defined as the norm on C^{PL}

Definition 3 Suppose $f \in C^{PL}$, the string energy is defined as:

$$E(f) = \langle f, f \rangle = \sum_{\{u, v\} \in K} k(u, v) \|f(u) - f(v)\|^2 \quad (2)$$

By changing the string constants $k(u, v)$ in the energy formula, we can define different string energies.

Definition 4 Suppose for edge $\{u, v\}$, it is shared by n tetrahedra thus it is against to n dihedral angles, $\theta_i, i = 1, \dots, n$. Define the parameters

$$k_{u, v} = \frac{1}{12} \sum_{i=1}^n l_i \cot(\theta_i) \quad (3)$$

where l_i is the length of edge to which edge $\{u, v\}$ is against in the domain manifold M . The string energy obtained is called the harmonic energy. The detailed explanation for the harmonic energy in \mathbb{R} can be found at Appendix.

Definition 5 The piecewise Laplacian is the linear operator $\Delta_{PL} : C^{PL} \rightarrow C^{PL}$ on the space of piecewise linear functions on K , defined by the formula

$$\Delta_{PL}(f) = \sum_{\{u, v\} \in K} k(u, v)(f(v) - f(u)) \quad (4)$$

If f minimizes the string energy, then f satisfies the condition $\Delta_{PL}(f) = 0$. Suppose M_1, M_2 are two meshes and the map $\vec{f} : M_1 \rightarrow M_2$ is a map from M_1 to \mathbb{R}^3 .

Definition 6 For a map $\vec{f} : M_1 \rightarrow \mathbb{R}^3$, $\vec{f} = (f_0, f_1, f_2)$, we define the energy as the norm of \vec{f} :

$$E(\vec{f}) = \|\vec{f}\|^2 = \sum_{i=0}^3 \|f_i\|^2 \quad (5)$$

The Laplacian is defined in a similar way.

Definition 7 For a map $\vec{f} : M_1 \rightarrow \mathbb{R}^3$, the piecewise Laplacian of \vec{f} is

$$\Delta_{PL}\vec{f} = (\Delta_{PL}f_0, \Delta_{PL}f_1, \Delta_{PL}f_2) \quad (6)$$

A map $\vec{f} : M_1 \rightarrow M_2$ is harmonic, if and only if it only has a normal component, and the tangential component is zero.

$$\Delta_{PL}(\vec{f}) = (\Delta_{PL}\vec{f})^\perp \quad (7)$$

2.2. Steepest Descent Method

Suppose we would like to compute a mapping $\vec{f} : M_1 \rightarrow M_2$ such that \vec{f} minimizes a string energy $E(\vec{f})$. This can be solved easily by the steepest descent algorithm:

$$\frac{d\vec{f}(t)}{dt} = -\Delta\vec{f}(t) \quad (8)$$

$\vec{f}(M_1)$ is constrained to be on M_2 , so $-\Delta\vec{f}$ is a section of M_2 's tangent bundle.

Based on the above definitions and algorithm, our volumetric harmonic brain mapping algorithm is given below.

Algorithm 1 Volumetric Harmonic Mapping

Input (mesh M , step length δt , energy difference threshold δE),

output ($\vec{h} : M \rightarrow D^3$), where \vec{h} is a harmonic map.

1. Compute the surface structure, ∂M , of the mesh M . Compute its conformal mapping to the surface of a sphere, $\vec{g} : \partial M \rightarrow S^2$ [3, 4];
2. For each boundary vertex, $v, v \in \partial M$, let $\vec{h}(v) = \vec{g}(v)$; for each interior vertex, $v, v \in M \setminus \partial M$, let $\vec{h}(v) = (0, 0, 0)$, compute the harmonic energy E_0 ;
3. For each interior vertex, $v \in M \setminus \partial M$, compute its derivative $D\vec{h}$;
4. Update $\vec{h}(v)$ by $\delta\vec{h}(v) = -D\vec{h}(v)\delta t$;
5. Compute the harmonic energy E ;
6. If $E - E_0 < \delta E$, return \vec{h} . Otherwise, assign E to E_0 and repeat steps 3 through 6.

3. EXPERIMENTS

In our experiments, we use tetrahedra to represent the volume data. We tested our algorithm on both synthetic and brain volume data. Our synthetic data is a cube consisting of many tetrahedra. Figure (a) shows a cube in wireframe mode and (b) shows the solid sphere onto which it harmonically mapped. We also performed some experiments to study the harmonic map obtained. As shown in Figure 1(c) and (d), we assign a random color to each vertex of the cube

model. We then removed some tetrahedra from the cube. We also remove these tetrahedra from the sphere. Since the cube has a convex surface, this shows that the mapping is a smooth bijection, i.e. diffeomorphism. Figure 1(e) and (f) shows another experiment. We started with a different surface condition (different conformal map on the surface via Möbius transformation). The harmonic map changes. We embedded the bunny in the resulting using its barycentric coordinate. As expected, the bunny was severely distorted, showing that the adjusted boundary mapping is propagated to the interior as well.

Methods to tetrahedralize the brain for FEM analysis are somewhat rare in the literature, although they are used occasionally for surgical simulation, or mapping intraoperative brain change. In our current experiments, we apply the technique developed in [1] to brain image tetrahedralization problem. This algorithm is called sphere carving algorithm. The input images to this algorithm are a sequence of binary 3D volumetric brain images which result from applying a Gaussian mixture tissue classifier to an MRI, in order to classify each pixel as white matter (in this case, for illustration purposes) and non-white matter. Figure 1(g) shows a few sections from this binary volume. Our goal is to build a tetrahedral brain volume while maintaining a genus zero surface. The sphere carving algorithm [1] takes a sequence of brain MRI images. First it builds a large sphere tetrahedral mesh which totally encloses the brain 3D volume. Then it keeps removing the tetrahedra outside of the brain volume while maintaining a genus zero surface. It outputs a brain tetrahedral mesh with a genus zero boundary.

To reduce memory requirements in the implementation, we use a multi-resolution method to represent the brain volume data. A coarse-scale brain model (which could be further refined) is shown in Figure 1(i) and (j). The volumetric brain harmonic mapping result is shown in Figure 1(k) and (l). We show this result at coarse scale to visualize the solution grid, but it can be further refined to capture greater geometric detail.

4. CONCLUSION AND FUTURE WORK

This paper introduces a novel volumetric brain mapping method. First we map the volumetric boundary conformally onto a sphere. Then with this boundary condition, we compute its harmonic map in the object interior with a heat flow method. Our work is general enough to be easily generalized to higher dimensional cases, or to other organ systems than brain, e.g. for representing cardiac motion. To apply this algorithm on brain mapping problem, we developed a novel algorithm to calculate the simplicial decomposition of volume adapted to surface. Our experimental results on both synthetic and brain MRI image data are promising.

Since the exterior brain surface is highly convoluted, computation of 3D harmonic maps is difficult. In the future, we will study the necessary and sufficient conditions for a 3D harmonic map to be diffeomorphic. We will also use non-structured tetrahedral mesh to represent brain volumetric data and test our algorithm on it.

5. REFERENCES

- [1] Y. Wang, X. Gu, and S.T. Yau, "Volumetric harmonic mapping," in *Communications in Information and Systems*, 2003.
- [2] P.M. Thompson and A.W. Toga, "A framework for computational anatomy," in *Computing and Visualization in Science*, 2002, vol. 5, pp. 1–12.
- [3] X. Gu, Y. Wang, T. Chan, P.M. Thompson, and S.-T. Yau, "Genus zero surface conformal mapping and its application to brain surface mapping," in *Information Processing in Medical Imaging*, Ambleside, UK, July 2003, pp. 172–184.
- [4] Y. Wang, X. Gu, T. Chan, P.M. Thompson, and S.-T. Yau, "Intrinsic brain surface conformal mapping using a variational method," in *SPIE International Symposium on Medical Imaging*, 2004.
- [5] P.M. Thompson and A.W. Toga, "A surface-based technique for warping 3-dimensional images of the brain," *IEEE Transactions on Medical Imaging*, vol. 15, no. 4, pp. 1–16, August 1996.
- [6] G.E. Christensen, S.C. Joshi, and M.I. Miller, "Volumetric transformation of brain anatomy," *IEEE Transactions on Medical Imaging*, vol. 16, no. 6, pp. 864–877, December 1997.
- [7] J.C. Gee, "On matching brain volumes," *Pattern Recognition*, vol. 32, pp. 99–111, 1999.
- [8] M. Ferrant, S.K. Warfield, A. Nabavi, F.A. Jolesz, and R. Kikinis, "Registration of 3d intraoperative MR images of the brain using a finite element biomechanical model," in *MICCAI*, 2000, pp. 19–28.

APPENDIX

Proof of Equation 3

As shown in Figure 1(h), we define $\vec{s}_i = \text{Area}(\text{Face } i)\vec{n}_i$, $i = 1, 2, 3, 4$, where \vec{n}_i is the normal on Face i . Due to $(\vec{s}_i) = -\sum_{j \neq i} \langle \vec{s}_j, \vec{n}_i \rangle$, and \vec{n}_i , $i = 1, 2, 3, 4$ can uniquely determine a frame in the space, we have $\sum_{i=1}^4 \vec{s}_i = 0$ and $\langle \vec{s}_i, \vec{s}_i \rangle = -\sum_{i \neq j} \langle \vec{s}_i, \vec{s}_j \rangle$, $i = 1, 2, 3, 4$. For a random point \vec{r} inside the tetrahedron, its barycentric coordinate is $\vec{r} = \sum_{i=1}^4 (\lambda_i \vec{p}_i)$, where $\lambda_i = \frac{1}{3} \frac{\langle \vec{r}, \vec{s}_i \rangle}{V}$, where V is the volume of tetrahedron. For a function defined on the tetrahedron, $f(\vec{r}) = \sum_{i=1}^4 \lambda_i f(\vec{p}_i) = \sum_{i=1}^4 \frac{1}{3} \frac{\langle \vec{r}, \vec{s}_i \rangle}{V}$. Thus we have $\nabla f = \frac{1}{3V} \sum_{i=1}^4 \vec{s}_i f_i$. We also can see The harmonic energy for the tetrahedron can be computed as

$$\begin{aligned}
 E(f) &= \frac{V}{2} \langle \nabla f, \nabla f \rangle = \frac{1}{18V} \left\langle \sum_{i=1}^4 \vec{s}_i f_i, \sum_{i=1}^4 \vec{s}_i f_i \right\rangle \\
 &= \frac{1}{18V} \left(\sum_{i=1}^4 \langle \vec{s}_i, \vec{s}_i \rangle f_i^2 + 2 \sum_{i \neq j} \langle \vec{s}_i, \vec{s}_j \rangle f_i f_j \right) \\
 &= - \sum_{i \neq j} \frac{\langle \vec{s}_i, \vec{s}_j \rangle}{18V} (f_i - f_j)^2 \\
 &= \sum_{\substack{i \neq j, p \neq q \\ \{p, q\} = I \setminus \{i, j\}}} l_{pq} \frac{\cot(\theta_{pq})}{12} (f_i - f_j)^2
 \end{aligned} \tag{9}$$

where $I = \{1, 2, 3, 4\}$, $\frac{\langle \vec{s}_i, \vec{s}_j \rangle}{V} = -\frac{|\vec{s}_i| \frac{1}{2} l_{pq} h_q \cos(\theta_{pq})}{\frac{1}{3} |\vec{s}_i| h_q \sin(\theta_{pq})} = -\frac{3}{2} l_{pq} \cot(\theta_{pq})$, where l_{pq} and h_q are the edge length and height length in triangle q , as shown in Figure 1(h). The proof is general and it can be easily generalized to higher dimensional cases.

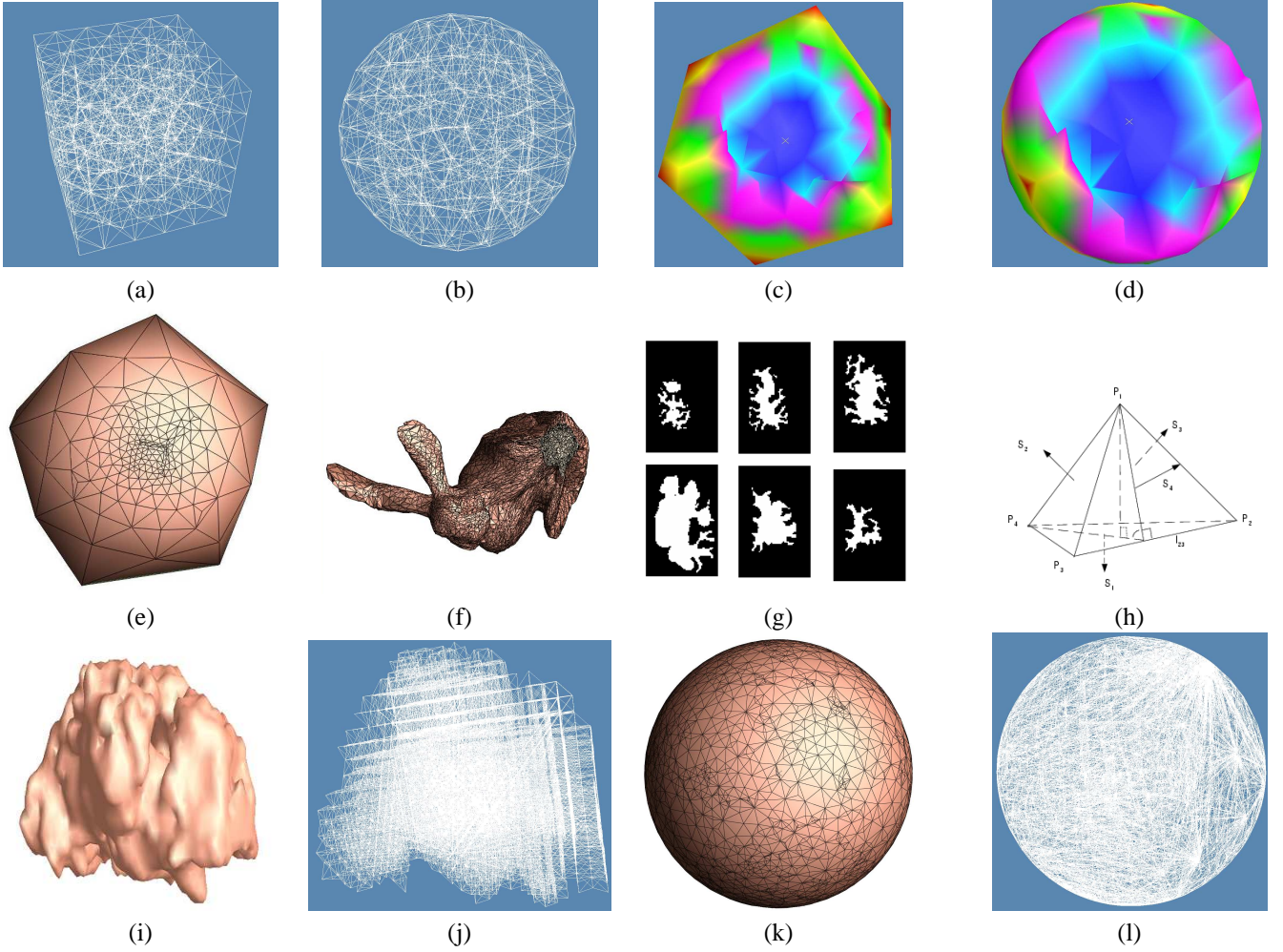


Fig. 1. (a) is a volumetric cube. (b) is its harmonic map onto a solid sphere, both of them are shown in wireframe mode. (c) and (d) illustrates the interior of the cube and its map onto a solid sphere. We plot random colors inside the cube and take some tetrahedra out of the cube (c). (d) shows the internal geometry after we removed the same tetrahedra from the solid sphere. This illustrates how the bijection maps simply connected regions to simply connected regions of the sphere, and points in the two coordinate systems can be associated. (e) and (f) illustrates how a boundary condition affects the harmonic map. We embedded a bunny inside a cube and got the harmonic map of the cube onto the solid sphere. After we change the boundary condition, we get a new harmonic map. (e) shows the new boundary condition. (f) shows the distorted bunny embedded in the solid sphere, which indicates the difference between different harmonic maps. (g) shows some binary brain images, where white pixels are brain's white matter, and black pixels are non-white matter. (h) illustrates a tetrahedron. (i) is a boundary surface of a brain volume. The brain volume is shown in (j) in wireframe. We get a harmonic map of the brain onto a solid sphere. (k) is the boundary surface of the solid sphere and (l) is the solid sphere in wireframe mode. The resulting embedding can be used to induce a canonical spherical coordinate system for the brain interior.